G. G. HIRS
Research Engineer,
The Institute T. N. O.
for Mechanical Constructions,
Delft, Holland

Externally Pressurized Bearings With Inherent Friction Compensation

Inherent friction compensation can be obtained by grooving one of the bearing surfaces in such a way that the through-flow of lubricant (oil or gas) exerts viscous forces in the direction of motion. In this study, theoretical and experimental data have been presented and many applications suggested. An experiment concerning an application as a continuous viscometer has been successful.

MANY machines and devices contain running elements whose energy consumption is largely due to friction losses (heat generation) in the bearings. The external drive starts up the element, or provides other changes of speed, and yields an energy output just equal to the friction loss while the element runs at a constant speed.

Externally pressurized bearings provide a means of keeping the friction loss to a minimum. The pressurization, however, demands a constant flow of a high-pressure fluid, thereby necessitating a pump or a compressor. If a pump or a compressor has to be installed for the benefit of the bearing operation only, one will try to eliminate such special equipment by reconsidering the drawbacks of the application of self-acting or rolling-element bearings.

The externally pressurized bearings, to be dealt with in this study, still need a pump or a compressor. However, the external drive can be eliminated by transferring the driving action to the bearings.

Inherent friction compensation in the bearings can be obtained by grooving one of the mating surfaces in such a way that the outflowing fluid has a component in the direction of motion.

Applications of these bearings may well lie in the field of running belts, tape, paper, film or foils, gyroscopes, centrifuges, memory drums, machine beds, and hydraulic or pneumatic controls. An experiment concerning an application as a continuous viscometer has been successful.

Pressure Buildup

We assume the lubricant to be noncompressible and apply other assumptions usual in bearing analysis, so that the Navier-Stokes equations reduce to

$$\frac{\partial p}{\partial x} = \eta \frac{\partial^2 v_x}{\partial z^2} \tag{1}$$

and

$$\frac{\partial p}{\partial y} = \eta \frac{\partial^2 v_y}{\partial z^2} \tag{2}$$

The journal is expected to be run in a central position. The pressure buildup is shown in Fig. 1. The coordinate system is connected to the grooved surface. The groove shape need not be defined at this stage; h is a wavelike function of y, $h_{\min} = h_0$.

From (1) and (2) it follows that, respectively,

$$v_x = \frac{-1}{2\eta} \frac{\partial p}{\partial x} z(h - z) - v \frac{h - z}{h} \cos \alpha \tag{3}$$

$$v_y = \frac{-1}{2\eta} \frac{\partial p}{\partial y} z(h - z) + v \frac{h - z}{h} \sin \alpha \tag{4}$$

The volume flows per unit of width are

$$Q_x = \frac{-1}{12\eta} \frac{\partial p}{\partial x} h^3 - \tfrac{1}{2} v h \cos \alpha \tag{5}$$

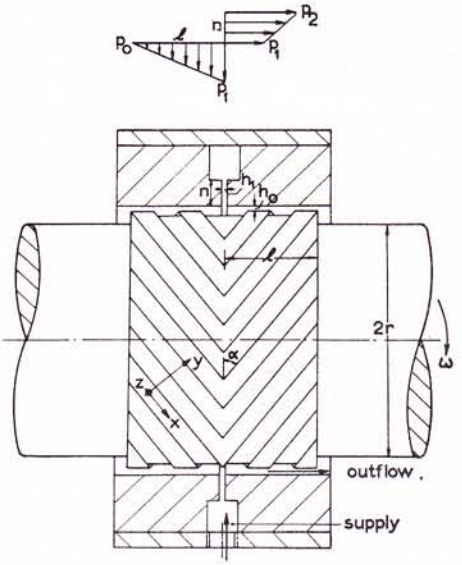

Fig. 1 Externally pressurized bearing with inherent friction compensation

Contributed by the Applied Mechanics Division for publication in the JOURNAL OF APPLIED MECHANICS.

Discussion of this paper should be addressed to the Editorial Department, ASME, United Engineering Center, 345 East 47th Street, New York, N. Y. 10017, and will be accepted until July 10, 1965. Discussion received after the closing date will be returned. Manuscript received by ASME Applied Mechanics Division, April 24, 1964. Paper No. 65—APM-B.

Nomenclature

p, p_0, p_1, p_2 = pressure
x, y, z = coordinates connected to grooved surface
η = viscosity (dynamic)
v_x, v_y, v = velocity
h, h_0 = film thickness
Q_x, Q_y, Q_t = volume flow per unit of width
m = subscript (mean)
l, n = length
α = lead angle
N = available power per unit of area; heat generation per unit of area
$P = \dfrac{(p_1 - p_0)h_0^2}{\eta v l}$ = dimensionless number
$H = h/h_0$ = dimensionless number
τ_x, τ_y, τ = viscous force per unit of area
ν = viscosity (kinematic)
ω = angular speed (rad/sec)
r = radius

$$Q_y = \frac{-1}{12\eta}\frac{\partial p}{\partial y}h^3 + \tfrac{1}{2}vh\sin\alpha \qquad (6)$$

Next we assume the number of grooves to be very great. With reference to the law of continuity of flow, it can be established that $\frac{\partial p}{\partial x}$ is constant in y and x-directions:

$$\frac{\partial p}{\partial x} = \frac{p_1 - p_0}{l}\sin\alpha$$

The mean flow over one wavelength (dam and groove) is

$$(Q_x)_m = \frac{-1}{12\eta}\frac{(p_1 - p_0)\sin\alpha}{l}(h^3)_m + \tfrac{1}{2}v(h)_m\sin\alpha \qquad (7)$$

It can be established also that a pressure rise in the y-direction can be separated into a wavelike function of y, and a gradient which is constant over y and x:

$$\left(\frac{\partial p}{\partial y}\right)_m = \frac{p_1 - p_0}{l}\cos\alpha$$

and that Q_y is constant.

From

$$Q_y = \frac{-1}{12\eta}\frac{\partial p}{\partial y}h^3 + \tfrac{1}{2}vh\sin\alpha$$

it follows that

$$Q_y(1/h^3)_m = \frac{-1}{12\eta}\left(\frac{\partial p}{\partial y}\right)_m + \tfrac{1}{2}v(1/h^2)_m\sin\alpha$$

or

$$Q_y = \frac{-1}{12\eta}\frac{p_1 - p_0}{l}\frac{1}{(1/h^3)_m}\cos\alpha + \tfrac{1}{2}v\frac{(1/h^2)_m}{(1/h^3)_m}\sin\alpha \qquad (8)$$

The outflow per unit of width in an axial direction ($Q_l = (Q_x)_m\sin\alpha + Q_y\cos\alpha$) is

$$Q_l = \frac{-1}{12\eta}\frac{p_1 - p_0}{l}\left\{(h^3)_m\sin^2\alpha + \frac{1}{(1/h^3)_m}\cos^2\alpha\right\} - \tfrac{1}{2}v\left\{(h)_m - \frac{(1/h^2)_m}{(1/h^3)_m}\right\}\sin\alpha\cos\alpha \qquad (9)$$

Using this formula, we can obtain an expression for the available power per unit of area of the mating surfaces:

$$N = \frac{p_1 - p_0}{l}Q_l$$

After introducing the dimensionless numbers

$$P = \frac{(p_1 - p_0)h_0^2}{\eta v l} \text{ and } H = \frac{h}{h_0}$$

it follows that

$$\frac{Nh_0}{\eta v^2} = \tfrac{1}{2}P\left\{H_m - \frac{(1/H^2)_m}{(1/H^3)_m}\right\}\sin\alpha\cos\alpha + \frac{1}{12}P^2\left\{(H^3)_m\sin^2\alpha + \frac{1}{(1/H^3)_m}\cos^2\alpha\right\} \qquad (10)$$

For the case where v is zero, another dimensionless equation can be obtained:

$$\frac{N}{(p_1 - p_0)^2}\frac{\eta l^2}{h_0^3} = \frac{1}{12}\left\{(H^3)_m\sin^2\alpha + \frac{1}{(1/H^3)_m}\cos^2\alpha\right\} \qquad (11)$$

In the foregoing treatment, we did not deal with the supply of the lubricant. In Fig. 1, the fluid has been assumed to enter the bearing via a line source. The supply should amount to

$$2Q_l = \frac{1}{12\eta}\frac{p_z - p_1}{n}h_1^3 \qquad (12)$$

The film thickness, h_1, should be dimensioned in such a way that

$$p_1 \approx \frac{p_2 + p_3}{2}$$

in order to obtain a favorable load-carrying capacity and good stability characteristics.

This is a rough estimate; calculations on these properties are still in progress.

Expressions (10) and (11) are valid also for a finite number of grooves, by making allowance for an edge effect, which can be kept quite small; see Muijderman[1] on self-acting grooved bearings.

Note that Fig 1 shows a journal bearing; the foregoing calculation is, however, valid also for the case where the mating surfaces are of the radial-face type as in grooved thrust bearings.

Viscous Heat Generation

The reduced expression for the viscous heat generation in an element is

$$\eta\left(\frac{\partial v_x}{\partial z}\right)^2 + \eta\left(\frac{\partial v_y}{\partial z}\right)^2$$

The viscous heat generation per unit of area over the mating surfaces is

$$N = \int_0^h \left\{\eta\left(\frac{\partial v_x}{\partial z}\right)^2 + \eta\left(\frac{\partial v_y}{\partial z}\right)^2\right\}dz \qquad (13)$$

Gradients $\partial v_x/\partial z$ and $\partial v_y/\partial z$ can be derived from (3) and (4); we obtain an expression in which h and $\partial p/\partial y$ appear, both of which are still dependent on y.

The mean viscous heat generation per unit of area is found by inserting $\partial p/\partial y$, as a result of equating (6) and (8), and by averaging all functions of h.

The resulting expression in dimensionless form reads

$$\frac{Nh_0}{\eta v^2} = (1/H)_m + 3\left\{(1/H)_m - \frac{(1/H^2)_m^2}{(1/H^3)_m}\right\}\sin^2\alpha + \frac{1}{12}P^2\left\{(H^3)_m\sin^2\alpha + \frac{1}{(1/H^3)_m}\cos^2\alpha\right\} \qquad (14)$$

By equating (10) and (14), we obtain

$$P = 2\frac{(1/H)_m + 3\left\{(1/H)_m - \dfrac{(1/H^2)_m^2}{(1/H^3)_m}\right\}\sin^2\alpha}{\left\{H_m - \dfrac{(1/H^2)_m}{(1/H^3)_m}\right\}\sin\alpha\cos\alpha} \qquad (15)$$

By equating (10) and (14), we have implicitly stated that all available energy is transformed into viscous heat, and it should be possible to obtain the same expression for P by stating that the viscous forces in the direction of motion exerted on the moving member are zero.

The viscous force can be derived from

$$\tau_x = \eta\left(\frac{\partial v_x}{\partial z}\right)_{z=0} \quad \text{and} \quad \tau_y = \eta\left(\frac{\partial v_y}{\partial z}\right)_{z=0}$$

[see expressions (3) and (4)].

In the resulting formulas, two symbols that are dependent on y appear, namely, h and $\partial p/\partial y$.

The mean viscous force per unit of area in x and y-directions is found by inserting $\partial p/\partial y$, as a result of equating (6) and (8), and by averaging all functions of h.

The viscous force in the direction of motion τ_m is

$$\tau_m = (\tau_x)_m\cos\alpha - (\tau_y)_m\sin\alpha$$

[1] E. A. Muijderman, "Spiral Groove Bearings," doctoral thesis. published by Philips Research Laboratories, Eindhoven, The Netherlands, 1963.

and thus

$$\tau_m = \frac{1}{2}\,\frac{p_1 - p_0}{l}\left\{h_m - \frac{(1/h^2)_m}{(1/h^3)_m}\right\}\sin\alpha\cos\alpha$$
$$-\eta v\,(1/h)_m - 3\eta v\left\{(1/h)_m - \frac{(1/h^2)_m{}^2}{(1/h^3)_m}\right\}\sin^2\alpha \quad (16)$$

Equation (16) for $\tau_m = 0$ and (15) are identical. Equation (16) also gives a dimensionless expression for the viscous force while $v = 0$:

$$\frac{\tau_m}{p_1 - p_0}\,\frac{l}{h_0} = \frac{1}{2}\left\{H_m - \frac{(1/H^2)_m}{(1/H^3)_m}\right\}\sin\alpha\cos\alpha \quad (17)$$

Optimized Parameters

Two criteria in optimizing parameters are given:

(*a*) For a bearing of given configuration and lubricant, the maximum speed should be run with a minimum energy consumption. After inserting (15) into (14), we obtain

$$\frac{Nh_0}{\eta v^2} = (1/H)_m + 3\left\{(1/H)_m - \frac{(1/H^2)_m{}^2}{(1/H^3)_m}\right\}\sin^2\alpha$$
$$+\frac{1}{3}\left[\frac{(1/H)_m + 3\left\{(1/H)_m - \frac{(1/H^2)_m{}^2}{(1/H^3)_m}\right\}\sin^2\alpha}{\left\{H_m - \frac{(1/H^2)_m}{(1/H^3)_m}\right\}\sin\alpha\cos\alpha}\right]^2$$
$$\left\{(H^3)_m\sin^2\alpha + \frac{1}{(1/H^3)_m}\cos^2\alpha\right\} \quad (18)$$

The criterion is satisfied by finding the minimum value of

$$\frac{Nh_0}{\eta v^2}$$

being dependent on dimensionless groove parameters. The treatment is restricted to grooves of a rectangular cross section (see Fig. 2 for dimensionless parameters). A general expression for the functions of the dimensionless film thickness is

$$(H^n)_m = 1 - \gamma + \gamma\delta^n$$

(*b*) For a bearing of given configuration and lubricant, the viscous force in the direction of motion, while not moving, should require a minimum energy consumption.

By combining equations (17) and (11), we obtain

$$\frac{\tau_m{}^2 h_0}{N\eta} = 3\,\frac{\left\{H_m - \frac{(1/H^2)_m}{(1/H^3)_m}\right\}^2\sin^2\alpha\cos^2\alpha}{(H^3)_m\sin^2\alpha + \frac{1}{(1/H^3)_m}\cos^2\alpha} \quad (19)$$

The criterion is satisfied by finding the maximum value of

$$\frac{\tau_m{}^2 h_0}{N\eta}$$

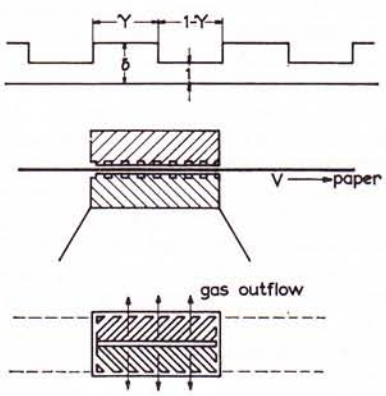

Fig. 2 Groove shape

Fig. 3 Bearing friction compensation for paper transport

Table 1 Optimized parameters

$Nh_0/\eta v^2$	δ	γ	$tg\alpha$	P
13.33	2	0.723	0.712	6.28
3.00	3	0.839	0.528	1.82
1.46	4	0.897	0.437	0.89
0.65	6	0.948	0.347	0.36

being dependent on dimensionless groove parameters. It can be shown that the groove should be rectangular for this case; the evidence will be given as part of a future paper on the optimization of grooved bearings and seals.

Both $Nh_0/\eta v^2$ and $\tau_m{}^2 h_0/N\eta$ are dependent on three dimensionless groove parameters γ, δ, and α as shown in Fig. 2 for the case of a rectangular groove. The formulas were programmed for a digital computer, and minimum values for (18) as well as one maximum value for (19) could be found with the aid of a standard program, minimizing a continuous nonlinear function of up to six independent variables by a refined gradient technique; see J. R. Dickinson.[2]

The maximum value of $\tau_m{}^2 h_0/N\eta = 0.197$ for $\gamma = 0.850$, $\delta = 6.19$, and $\tan\alpha = 0.424$.

The number $Nh_0/\eta v^2$ asymptotically reaches a minimum value of zero for $\delta \to \infty$, and therefore $P \to 0$. The number P, however, must not be zero, since it determines the load capacity and the stability of operation. In order to obtain nonzero values for P, we chose fixed values for δ and looked for the minimum value of $Nh_0/\eta v^2$. The results are shown in Table 1.

It is evident that the values of $Nh_0/\eta v^2$ are small enough. This fact can be made clear by comparing the total energy consumption of nongrooved and grooved hydrostatic bearings. The expression for the grooved bearing (14) reduces to a formula for the nongrooved bearing by inserting $H = 1$:

$$\frac{Nh_0}{\eta v^2} = 1 + \frac{1}{12}P^2$$

and thus the total energy consumption will be of the same order of magnitude in hydrostatic bearings, independent of whether the friction has been compensated for or not.

Applications

Applications of these bearings may well lie in the field of running belts, tape, paper, film or foils, gyroscopes, centrifuges, memory drums, machine beds, and hydraulic or pneumatic controls.

Belts, tape, paper, film, and *foils* can be supported (or guided) and driven at the same time, while the respective moving surfaces are separated by a gas or a liquid, Fig. 3, so that there will be no wear.

Destruction of the running material will also be avoided, because inertial forces in the material cannot be attributed to the drive and because the drive will exert no force at all when the material runs at its maximum speed.

It is probable that the device in Fig. 3 requires gas lubrication; our theory will need to be extended for that case.

A problem to be solved is the guiding of tape, and so on, in its plane perpendicular to the direction of motion; it is probable that a stabilizing effect can be obtained by applying nonconstant groove parameters.

Gyroscopes, centrifuges, memory drums, and *machine beds* can be provided with radial bearings, as in Fig. 1, and/or equivalent thrust bearings, thus eliminating the need for an external drive. Memory drums can be exchanged for memory foils of circular or cylindrical configuration. As they are nearly weightless, they can be accelerated very rapidly.

Pneumatic and hydraulic controls: The device as in Fig. 1 can be regarded as a means of control; pressure and/or viscosity de-

[2] J. R. Dickinson, "Computer Program for System Optimization," *Transactions of the Engineering Institute of Canada,* vol. 2, 1958, pp. 157–161.

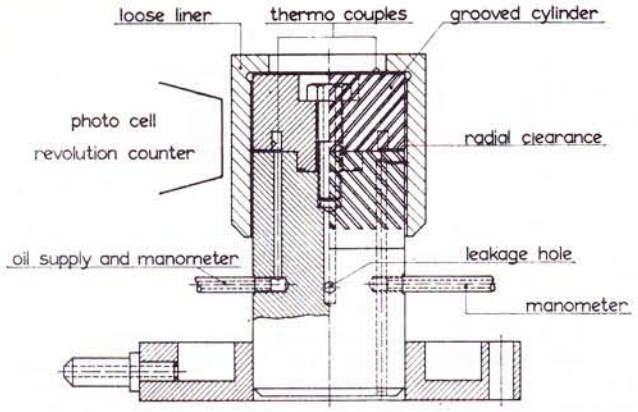

Fig. 4 Experimental viscometer

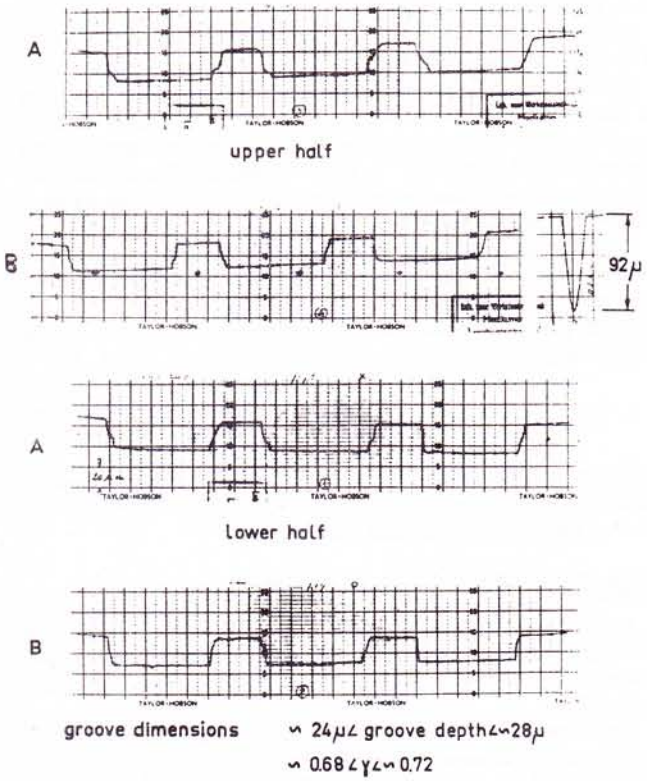

Fig. 5(a) Parameters of viscometer

termine a surface speed, a number of revolutions, and/or a torque (servomotors). It also can be applied as a means of measuring pressure or viscosity.

Experimental Viscometer

The theory presented in the preceding sections has been checked by means of an experimental viscometer, Fig. 4. The purpose of the instrument is to provide a simple and continuous measurement of the viscosity of a through-flow of liquid. The flow can be kept quite small. The liquid should be Newtonian. The operation is self-evident; theory predicts that

$$\frac{p_1 - p_0}{\eta\omega}$$

should be of a constant value for the case of an instrument of given dimensions and parameters. The dimensions of the instrument are shown in Fig. 5.

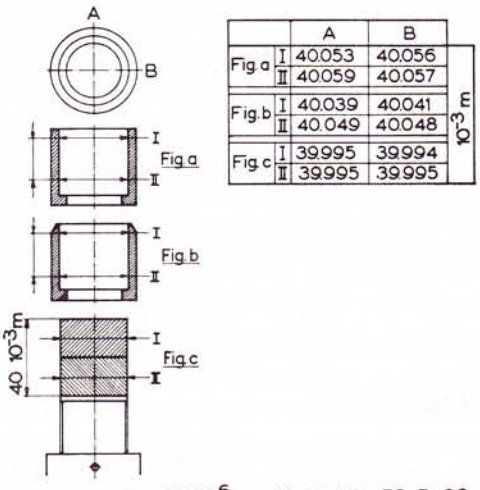

		A	B
Fig.a	I	40.053	40.056
	II	40.059	40.057
Fig.b	I	40.039	40.041
	II	40.049	40.048
Fig.c	I	39.995	39.994
	II	39.995	39.995

10^{-3} m

a and c: $h_0 \approx 31\ 10^{-6}$m $1.8 < \delta < 1.9$ $7.6 < P < 9.6$

b and c: $h_0 \approx 25\ 10^{-6}$m $2.0 < \delta < 2.1$ $5.3 < P < 6.5$

$\tan\alpha = 0.72$

Fig. 5(b) Parameters of viscometer

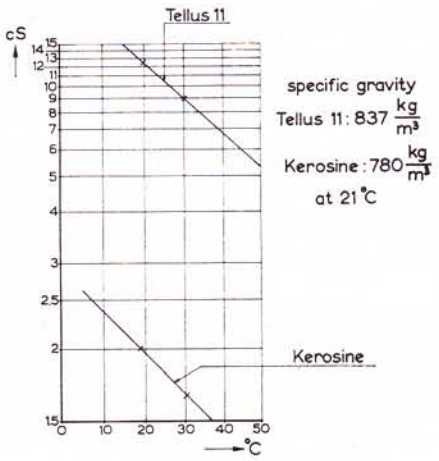

Fig. 6 Viscosities

The grooves were made by masking the ground cylinder, hard-chromium plating the unmasked area, removing masking, and grinding to a constant groove depth. The design parameters (see first row of Table 1) and the eventual parameters show considerable deviations. The eventual parameters and their scatter also appear in Fig. 5. They have been inserted into expression (15). The maximum and minimum values are shown in Fig. 5.

A comparison of Figs. 1 and 4 shows that these numbers are not yet relevant to the viscometer. The loose bearing liner of the viscometer requires a thrust collar. Accordingly, the viscous friction will be higher than allowed for, while the through-flow of lubricant will be smaller. The determination of the influence of the thrust collar is rather lengthy; it can be shown that the correction to P is smaller than 1 percent for the case of this viscometer at a pressure drop $(p_1 - p_0)$ of several atmospheres or more.

So far, two oils have been tested. A lubricant pump supplied the viscometer with oil. The pressures before and after the radial restriction were measured by means of strain-gage manometers. The number of revolutions follows from a photocell and electronic counter. The temperature of the oil was measured before entering and after leaving the restrictions of the viscometer, Fig. 4. The viscosity of both oils was measured by means of a Vogel-Ossag viscometer at about 20 and 30 C, Fig. 6. The experimental results are given in Tables 2–5. The last column shows the experimental dimensionless numbers P. They are somewhat higher than the numbers following from the theoretical treatment. The

Table 2 Experimental results with Tellus 11, elements (a) and (c), Fig. 5(b)

p_1-p_o	p_2-p_o	T_i	T_o	T_m	freq.	ν	P
atm.g	atm.g	°C	°C	°C	Hz	cS	
2.65	3.24	22.5	27.1	24.8	1.31	10.56	8.74
2.74	3.38	23.3	27.3	25.3	1.41	10.41	8.53
2.77	3.47	23.8	28.3	26.0	1.44	10.20	8.60
2.78	3.51	24.3	28.7	26.5	1.46	10.00	8.69
2.80	3.56	24.3	28.7	26.5	1.48	10.00	8.65
4.55	5.86	25.5	29.8	27.7	2.52	9.59	8.60
4.57	6.00	25.9	30.0	27.9	2.54	9.53	8.63
4.57	6.07	25.9	30.4	28.2	2.57	9.44	8.61
4.60	6.07	26.2	30.5	28.3	2.59	9.41	8.62
4.62	6.98	26.7	30.9	28.8	2.63	9.26	8.67
4.66	7.00	26.9	31.1	29.0	2.65	9.20	8.72
6.49	8.96	28.5	32.9	30.7	3.89	8.79	8.67
6.44	8.96	28.9	33.5	31.2	3.91	8.74	8.61
6.43	8.96	29.6	33.9	31.8	3.96	8.46	8.77
6.41	8.94	30.0	34.2	32.1	3.98	8.38	8.77
6.41	8.93	30.1	34.2	32.1	4.00	8.36	8.75
7.99	12.0	32.6	37.7	35.1	5.31	7.77	8.85
7.97	12.0	33.1	37.5	35.3	5.33	7.71	8.85
7.94	12.0	33.4	37.7	35.6	5.35	7.62	8.90
7.91	12.0	33.7	38.1	35.9	5.35	7.53	8.97
7.74	11.8	34.2	38.4	36.3	5.37	7.44	8.85
7.75	11.9	34.3	38.6	36.4	5.39	7.42	8.86
7.76	11.9	34.4	38.8	36.6	5.41	7.36	8.91

Table 3 Experimental results with kerosene, elements (a) and (c), Fig. 5(b)

p_1-p_o	p_2-p_o	T_i	T_o	T_m	freq.	ν	P
atm.g	atm.g	°C	°C	°C	Hz	cS	
0.75	1.07	17.4	18.8	18.1	1.65	2.03	10.9
0.77	1.09	17.6	19.0	18.3	1.70	2.02	10.9
0.78	1.11	17.9	19.3	18.6	1.72	2.01	11.0
0.78	1.16	18.1	19.5	18.8	1.76	2.01	10.8
0.79	1.20	18.6	20.0	19.3	1.83	1.99	10.6
0.80	1.22	18.8	20.2	19.5	1.83	1.98	10.9
1.21	2.00	19.3	20.8	20.0	2.84	1.96	11.0
1.22	2.00	19.7	21.1	20.4	2.84	1.95	10.8
1.22	2.02	20.0	21.4	20.7	2.84	1.94	10.8
1.22	2.02	20.4	21.8	21.1	2.85	1.93	10.8
1.22	2.00	20.4	22.0	21.2	2.85	1.92	10.9
1.21	1.98	20.6	22.2	21.4	2.85	1.91	10.8
1.67	3.07	21.3	22.9	22.1	4.06	1.89	10.6
1.68	3.07	21.5	23.3	22.4	4.06	1.88	10.8
1.66	3.07	21.7	23.5	22.6	4.05	1.87	10.7
1.64	3.04	22.2	23.8	23.0	4.04	1.86	10.7
1.63	3.04	22.5	24.2	23.4	4.03	1.85	10.7
1.63	3.02	22.5	24.4	23.5	4.04	1.85	10.7
2.25	4.84	24.2	26.2	25.2	5.83	1.79	10.5
2.22	4.82	24.7	26.6	25.7	5.79	1.78	10.5
2.20	4.80	25.1	27.0	26.0	5.80	1.77	10.5
2.19	4.80	25.5	27.5	26.5	5.81	1.76	10.5
2.19	4.78	25.5	27.5	26.5	5.79	1.76	10.5
2.75	7.16	27.8	30.2	29.0	7.57	1.69	10.5
2.67	7.07	28.7	30.9	29.8	7.49	1.67	10.5
2.60	7.02	29.3	31.6	30.5	7.43	1.65	10.4
2.55	6.96	29.8	32.3	31.1	7.37	1.64	10.3
2.53	6.93	30.5	32.9	31.7	7.34	1.62	10.4

author believes this to result from an eccentric running liner because of a nonconstant resistance of the radial restriction around the circumference. Other inconsistencies are expected to be caused by measuring errors and dust particles blocking the minor clearances.

The results of Tables 4 and 5 are closer to the theoretical values than those of Tables 2 and 3. The experimental values of Table 4 differ by less than 10 percent from those of Table 5 although the viscosity is more than five times higher in Table 4. Too-high experimental values of P in the case of kerosene, Tables 3 and 5, go hand in hand with higher-than-expected excess pressures ($p_2 - p_0$).

Table 4 Experimental results with Tellus 11, elements (b) and (c), Fig. 5(b)

p_1-p_o	p_2-p_o	T_i	T_o	T_m	freq.	ν	P
atm.g	atm.g	°C	°C	°C	Hz	cS	
2.96	3.58	22.3	21.3	21.8	1.01	11.1	7.83
2.66	2.96	20.0	18.6	19.3	0.9	12.71	6.90
2.47	2.98	20.5	19.3	20.0	0.84	12.5	6.99
2.36	2.64	20.6	19.8	20.2	0.83	12.4	6.82
2.36	2.67	20.9	19.9	20.4	0.84	12.3	6.80
2.35	2.67	22.0	20.7	21.4	0.85	11.8	6.97
5.25	5.98	24.4	25.7	25.0	2.19	10.5	6.78
5.24	6.02	25.9	25.2	25.5	2.24	10.35	6.71
5.22	6.02	26.8	25.3	26.0	2.27	10.2	6.70
5.27	6.07	27.1	25.9	26.5	2.31	10.0	6.78
5.27	6.09	27.5	26.1	26.8	2.32	9.88	6.83
7.59	8.96	29.1	27.8	28.4	3.57	9.38	6.73
7.56	8.96	29.7	28.1	28.9	3.61	9.23	6.74
7.49	8.93	30.2	28.6	29.4	3.64	9.12	6.71
7.49	8.91	32.4	29.2	30.8	3.67	8.64	7.02
7.45	8.89	32.7	32.0	32.4	3.72	8.32	7.14
9.48	11.9	34.9	33.6	34.3	5.40	7.94	6.57
9.38	11.9	35.8	34.0	34.9	5.56	7.82	6.41
9.37	11.9	36.3	34.5	35.4	5.58	7.68	6.50
9.22	11.8	37.3	35.6	36.4	5.59	7.42	6.60
9.20	11.8	37.6	35.6	36.6	5.61	7.38	6.60
9.17	11.8	38.0	36.4	37.1	5.67	7.28	6.60

Table 5 Experimental results with kerosene, elements (b) and (c), Fig. 5(b)

p_1-p_o	p_2-p_o	T_i	T_o	T_m	freq.	ν	P
atm.g	atm.g	°C	°C	°C	Hz	cS	
1.17	1.44	25.8	25.9	25.9	2.87	1.80	7.19
1.10	1.42	25.8	25.8	25.8	2.65	1.78	7.43
1.10	1.47	25.6	25.7	25.6	2.66	1.78	7.37
1.10	1.49	25.5	25.6	25.6	2.65	1.78	7.40
1.10	1.51	25.5	25.6	25.5	2.66	1.79	7.36
1.44	2.18	25.2	25.3	25.2	3.53	1.79	7.24
1.44	2.18	25.3	25.3	25.3	3.53	1.79	7.25
1.45	2.18	25.3	25.4	25.3	3.54	1.79	7.29
1.45	2.18	25.3	25.4	25.3	3.54	1.79	7.29
1.45	2.18	25.3	25.4	25.4	3.54	1.79	7.31
1.95	3.04	25.3	25.5	25.4	4.72	1.79	7.35
1.95	3.07	25.4	25.5	25.5	4.72	1.79	7.36
1.95	3.07	25.5	25.6	25.6	4.73	1.78	7.36
1.95	3.07	25.6	25.7	25.6	4.73	1.78	7.36
1.95	3.07	25.7	25.7	25.7	4.72	1.78	7.38
2.87	5.07	26.6	26.7	26.6	7.04	1.75	7.38
2.86	5.09	26.9	27.1	27.0	7.05	1.75	7.37
2.87	5.09	27.2	27.2	27.2	7.05	1.74	7.43
2.78	5.07	28.4	28.4	28.4	7.00	1.71	7.39
2.78	5.07	28.4	28.4	28.4	7.00	1.71	7.39
3.06	7.02	29.3	29.6	29.4	8.01	1.68	7.24
3.03	7.04	29.9	30.0	29.9	8.04	1.66	7.19
3.04	7.04	30.2	30.2	30.2	8.04	1.66	7.25
3.01	7.07	30.3	30.5	30.4	8.02	1.65	7.23
3.01	7.04	30.6	30.7	30.7	8.01	1.65	7.27

The general impression of this experiment is, however, that it provides a strong support for the foregoing theory.

Future experiments can be made more accurate by obtaining a constant temperature throughout the viscometer, by mounting a finer filter or applying greater clearances, by obtaining more accurate dimensions, and by improving the measuring accuracy.

Acknowledgments

This work is part of a research program on grooved bearings and grooved seals at the Institute T.N.O. for Mechanical Constructions. The author thanks Prof. H. Blok of The Technological University of Delft for his advice and interest.

Reprinted from June 1965
Journal of Applied Mechanics